Chemical Science

EDGE ARTICLE

View Article Online
View Journal | View Issue

Cite this: *Chem. Sci.*, 2016, **7**, 5448

DNA-mediated cell surface engineering for multiplexed glycan profiling using MALDI-TOF mass spectrometry†

Ziyi He, Qiushui Chen, Fengming Chen, Jie Zhang, Haifang Li and Jin-Ming Lin*

Received 16th January 2016
Accepted 4th May 2016

DOI: 10.1039/c6sc00215c

www.rsc.org/chemicalscience

Glycans are crucial for many key biological processes and their alterations are often a hallmark of disease. Thus, multiplexed and sensitive analysis of glycans is of intense interest. Here we report a novel approach using DNA-mediated cell surface engineering for glycan profiling by MALDI-TOF mass spectrometry (MS). Following lectin binding, DNA amplification and hybridization, glycans on the cell surface are specifically labeled by short DNA probes, which can be facilely released, ionized and detected in MALDI-TOF MS. This strategy converts the analysis of glycans to the detection of DNA probes, overcoming the complicated composition and low ionization efficiency of glycans, enabling *in situ* detection and facilitating multiplex analysis. The amplification procedure also improves the sensitivity. This approach has been applied to evaluate glycomic alterations in cancer cells and provided the intrinsic distribution of glycans in tissues using MALDI imaging mass spectrometry.

Introduction

Glycans, as one of the four basic components of cells, are covalent assemblies of sugars that either exist in free form or attach to proteins or lipids.[1] They decorate all eukaryotic cell surfaces and are crucial for many key biological processes.[2,3] The expression and structure of glycans are often aberrant in pathological states, and these alterations can be a hallmark of diseases.[4,5] Thus multiplexed, sensitive and reliable analysis of glycans is highly desirable, and facilitates the understanding of their specific roles in biological processes and provides information for disease prediction and diagnosis.[6]

To date, a series of approaches have been developed for glycan analysis, such as fluorescence imaging, use of microarrays, electrochemical biosensors and mass spectrometry.[7–11] In particular, mass spectrometry, as a powerful and promising technology, has been widely applied to the detection and identification of glycans because of its broad detection range, high mass resolution and capability for multicomponent analysis.[12] Nevertheless, the conventional MS based method for cell surface glycan analysis typically involves several steps, including cell lysis, molecule extraction and separation, enzymatic deglycosylation, glycan derivatization and MS analysis.[13] It offers multiple molecule-level information, but suffers from the drawbacks of time-consuming procedures, complicated data analysis and the requirement of a large numbers of cells. The spatial information of glycan expression is also limited due to the sample homogenization. Recently, combined with direct enzymatic releasing of *N*-lined glycans or photocleavable mass tags,[14,15] *in situ* analysis of glycans in cells or tissues has been achieved by matrix-assisted laser desorption/ionization mass spectrometry (MALDI-MS). Unfortunately, these methods either suffer from the loss of glycan groups during treatment or are limited to a lack of mass tags for multiplexing detection. Thus, the development of multiplexed and *in situ* methods for glycans present on the cell surface with a high sensitivity and specificity is still important.

In this study, a MALDI-TOF MS based approach is developed for the multiplexed profiling of cell surface glycans using a DNA-mediated cell surface engineering strategy. Lectins, as carbohydrate-binding proteins isolated from different organisms (mainly from plants), are used for the specific targeting of cell surface glycans.[16] We encode lectins with DNA primers, which can be utilized in the subsequent rolling circle amplification, producing long single-strand DNA (ss-DNA) with repetitive sequence units (Fig. 1a).[17] After hybridizing with complementary short DNA probes, the labeled cells are analyzed by MALDI-TOF MS. The hydrogen bonds in DNA duplexes are facilely broken under laser irradiation, which makes the short DNA probes detach from the cell surface and be detected by TOF-MS (Fig. 1b). Therefore we convert the analysis of glycans to the detection of DNA probes, overcoming the complicated composition and low ionization efficiency of glycans, and facilitating multiplex analysis. The amplification procedure also improves the sensitivity. This novel strategy is then applied to evaluate the alterations of *N*-glycans in cancer cells with multidrug

Department of Chemistry, Beijing Key Laboratory of Microanalytical Methods and Instrumentation, Tsinghua University, Beijing 100084, China. E-mail: jmlin@tsinghua.edu.cn

† Electronic supplementary information (ESI) available. See DOI: 10.1039/c6sc00215c

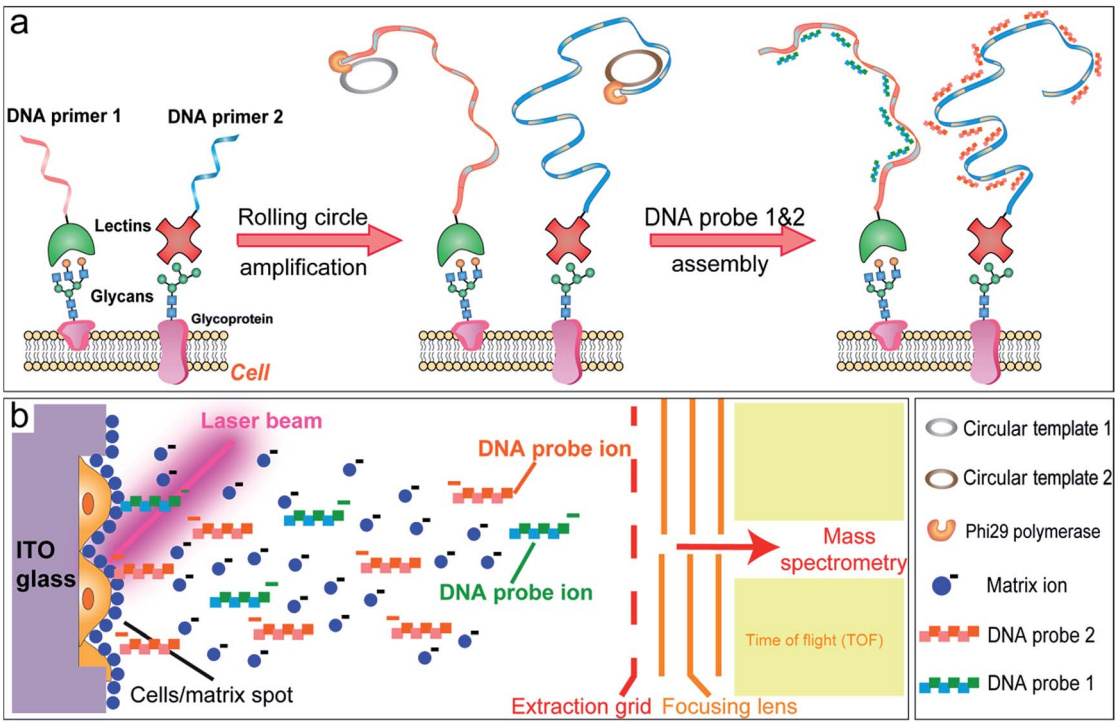

Fig. 1 Overview of the DNA-mediated cell surface engineering approach for multiplexed profiling of cell surface glycans using MALDI-TOF mass spectrometry. (a) Schematic illustration of the DNA-mediated cell surface engineering. (b) Cell surface glycan detection in MALDI-TOF MS. Laser irradiation easily led to the release, ionization and detection of the short DNA probes, whose MS signals represented the expression of corresponding glycans.

resistance and under drug stimuli. Owing to the preservation of spatial information, this robust approach can further be utilized in MALDI imaging mass spectrometry (MALDI-IMS), providing the intrinsic distribution of glycans in tissue sections.

Results and discussion

In the proof-of-concept experiments, we analyzed the α-D-mannosyl groups on the cell surface using concanavalin A (ConA), a lectin extracted from jack bean and binding specifically to the mannosyl and glucosyl groups. A covalent conjugation strategy was utilized for the coupling of ConA and the DNA primer.[18] As shown in Fig. 2a, a hydrazide moiety was firstly incorporated on ConA *via* reaction with the amino groups in lysine side chains. A ConA–DNA conjugate was then formed *via* a hydrazine linkage by the reaction of hydrazide groups and 5′-aldehyde modified DNA. The conjugation product was verified using microchip capillary electrophoresis (MCE). New bands with a lower mobility were clearly shown in the electrophoretogram (Fig. 2b), representing the ConA–DNA conjugates. To evaluate the recognition ability of the conjugates, cells were stained with FITC (fluorescein isothiocyanate)-labeled ConA–DNA conjugates. Flow cytometry analysis demonstrated a distinct fluorescence increase after labeling, which could be distinguished from cells treated with DNA-FITC and control cells (Fig. 2c). Free D-mannose and D-glucose inhibited the binding of ConA–DNA to the cell surface, while the nonspecific D-galactose showed no inhibition (Fig. S1†). This monosaccharide inhibition assay verified the recognition specificity of the ConA–DNA conjugates. Since there were no glucosyl group presented in the processed *N*-glycans, the mannosyl groups are the epitopes that were recognized by ConA–DNA on the cell surface.

Further, we used rolling circle amplification (RCA) to engineer long ss-DNA on the cell surface, by hybridizing the DNA primers with circular DNA templates and amplifying using Phi29 polymerase. This isothermal process preserved the integrity of the lectin–glycan complexes and led to a signal amplification. The RCA reaction of lectin–DNA conjugates in

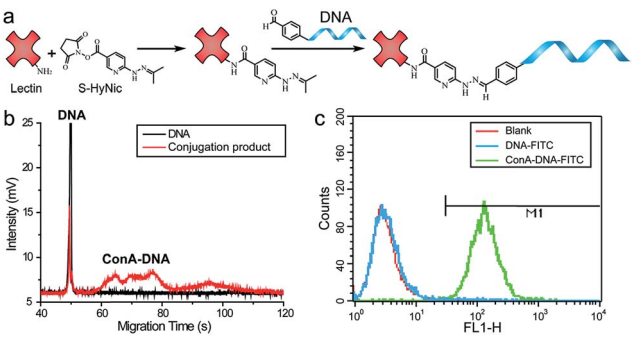

Fig. 2 Synthesis and evaluation of the ConA–DNA conjugate. (a) Coupling strategy for the synthesis of lectin–DNA conjugates. (b) Analysis of the conjugation by MCE; DNA in solution was stained with SYBR gold. (c) Flow cytometry analysis shows the binding of ConA–DNA-FITC (green) and DNA-FITC (blue) in cells. Untreated cells are shown in red for comparison.

solution was verified using agarose electrophoresis. New bands with more than 1000 bps in length were displayed, which were the bands of the RCA products (Fig. S2†). For *in situ* cell labeling and amplification, MCF-7 cells were firstly cultured on ITO glass, which was conductive, enabling subsequent MALDI-MS detection. High cell viability was demonstrated by live/dead assays after 2 days culturing (Fig. S3†). Cells were fixed, labeled by ConA–primer1 and the RCA reaction was performed. Then, we used the FITC-labeled short DNA probe1 for hybridization with the repetitive sequences in the RCA products. Confocal imaging showed that a strong fluorescence signal emanated from the cell surface, while negligible fluorescence was observed in the control experiments when the cells were incubated with non-specific BSA–primer1 or only the primer1 DNA and the RCA reaction was performed (Fig. 3). These results confirmed the specific binding, RCA reaction and probe hybridization directly on the cell surface.

After the cell surface engineering, ITO glass with cells was affixed onto the stainless steel MALDI plate by conductive tape, and MALDI-TOF MS was performed for glycan analysis. Matrix crystallization and homogeneity were critical factors, affecting the robustness and reproducibility of MS signals.[19] Here we chose 3-hydroxypicolinic acid (3-HPA) as the matrix and employed a home-made inkjet printing device for matrix introduction. An array of reproducible droplets was produced on the ITO glass, drying to form crystalline matrix spots of ~300 μm in diameter (Fig. S4a and b†). Under laser irradiation, the hydrogen bonds in DNA duplexes were easily broken, leading to the desorption and ionization of the short DNA probes. As shown in Fig. 4a, with specific ConA–primer1 labeling and RCA reaction, a prominent peak was observed in the mass spectrum, corresponding to the short DNA probe1 (Fig. S6a†). In contrast, no MS signal was detected in control experiments (Fig. 4b and c). The mass deviation between the molecular ion peak and the calculated molecular weight value (Table S1†) might be due to the shortened distance from the initial ionization position to the extraction grid when molecules were ionized from the ITO glass (detailed explanation is in the ESI†). The DNA amplification procedure increased the signal intensity nearly 10 fold compared to the cells without RCA reaction (Fig. 4d). This result indicated the feasibility of our DNA engineering strategy for MALDI-MS analysis, which was capable of detecting cell surface glycans *in situ* with high sensitivity and specificity.

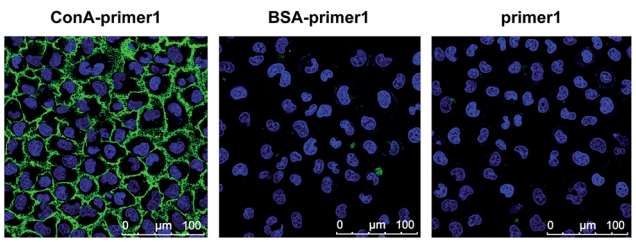

Fig. 3 Confocal images of cells labeled by ConA–primer1 (left), BSA–primer1 (middle) and primer1 (right), with RCA reaction performed and hybridized with FITC labeled DNA probe 1. DAPI was used as the nuclear stain (blue). The scale bars are 100 μm in all images.

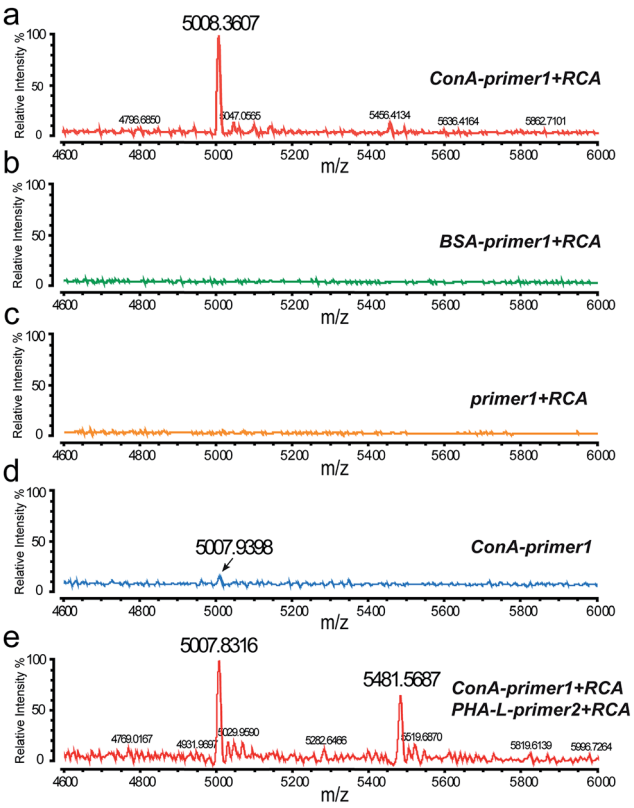

Fig. 4 MALDI-TOF MS analysis of the cell surface *N*-glycans based on DNA-mediated cell surface engineering. Mass spectrum of MCF-7 cells labeled by (a) ConA–primer1, (b) BSA–primer1, and (c) primer1, with RCA reaction performed and hybridized with DNA probe1. (d) Mass spectrum of cells labelled by ConA–primer1 and hybridized with DNA probe1 directly, without RCA reaction. (e) Multiplexed detection of cell surface *N*-glycans. Cells were co-labeled with ConA–primer1 and PHA-L–primer2, with RCA reaction performed, and hybridized with DNA probe1 and DNA probe2.

In this work, the approach of simultaneously labeling with different DNA sequences provides an opportunity for multiplexed analysis by mass spectrometry. To prove this concept, two types of lectins, ConA and PHA-L (*Phaseolus vulgaris* leucoagglutinin), were conjugated with two different DNA primers respectively and used for cell labeling. PHA-L was a lectin isolated from *Phaseolus vulgaris* and specifically recognized the β1-6GlcNAc (*N*-acetylglucosamine) branched *N*-glycan groups. After RCA reaction, two corresponding DNA probes modified with different fluorophores were added and hybridized on the cell surface. When analyzed in MALDI-MS, two obvious peaks of the DNA probes were demonstrated in the mass spectrum (Fig. 4e), corresponding to the expression of the two glycan groups. Confocal imaging was also used to confirm the multiplexed labeling, with strong green and red fluorescence emitted from the cell membrane (Fig. S5†).

We then applied this strategy to evaluate the alterations of *N*-glycans in cancer cells with multidrug resistance and under drug stimuli. Multidrug resistance, as a major problem in cancer chemotherapy, contributed to the failure of chemotherapeutic drug treatments.[20] Recent researches indicated that

aberrant glycan expression was correlated with cancer chemoresistance.[21] We analyzed the expressions of two types of *N*-glycans (α-D-mannosyl and β1-6GlcNAc groups) in the breast carcinoma cell line MCF-7 and its drug resistance cell line MCF-7/ADR using the MALDI-TOF MS based approach. We also profiled the glycan alterations in both cell lines under the treatment of tunicamycin (TM), which was an inhibitor of GlcNAc phosphotransferase, blocking the formation of *N*-glycosidic linkages in glycoprotein synthesis.[22] Owing to the matrix inhomogeneity, ion signals in MALDI-MS were always irreproducible, impeding its application in quantitative analysis. To solve this problem, we utilized the inkjet printing device to apply a DNA internal standard on cells prior to the matrix (Fig. S4c†), and the intensity ratio of the DNA probe to the internal standard was used in the subsequent semi-quantitative analysis (Fig. S6d†). As shown in Fig. 5a and b, the expressions of α-D-mannosyl and β1-6GlcNAc groups in MCF7/ADR cells were both higher than those in MCF7 cells. The elevated glycan expression might be due to the overexpression of P-glycoprotein in MCF-7/ADR cells. P-Glycoprotein, conferring resistance of cancer cells to a variety of chemotherapeutic drugs, was a heavily *N*-glycosylated transmembrane protein.[23] Thus its overexpression increased the expression of the *N*-glycans in cells. For drug treatment, the CCK-8 assay indicated that TM inhibited cell proliferation in a dose-dependant manner (Fig. S7†). Results of the MALDI-MS analysis demonstrated that the expressions of the two types of *N*-glycans both decreased with the increase of TM concentration, which was in good correlation with the standard flow cytometry analysis (Fig. S8†). Also, the drug resistant cell line MCF-7/ADR was more sensitive to TM, with a more pronounced downregulation of the *N*-glycans compared to MCF-7 cells at the same TM concentration. A previous study revealed that TM treatment could enhance the sensitivity of drug-resistant cancer cells to anticancer drugs.[24] We supposed that the glycomic alterations induced by TM might have a correlation with this reduction of multidrug resistance.

MALDI-IMS, as an important technology for tissue analysis, provides the intrinsic distribution and relative abundance of different compounds in tissue sections. Despite the recent advances in MALDI-IMS, it's still challenging to image some classes of molecules such as glycans and proteins, owing to their large molecule weights, reduced ionization efficiencies and complicated composition. Thus we further applied the DNA-mediated cell surface engineering strategy to MALDI-IMS to overcome these limitations. A human lung tumor tissue section was placed on ITO glass, labeled by ConA–primer1, amplified and hybridized with DNA probe1. The section was imaged at a spatial resolution of 200 μm. Fig. 5c showed the overall average mass spectrum of the imaged region, with a predominant peak at *m*/*z* 5006.51, corresponding to the DNA probe1. A mass spectrometric heat map was demonstrated in Fig. 5d, illustrating the spatial distribution of α-D-mannosyl groups in this tissue section. This result indicated the feasibility of our method in MALDI-IMS, which broadened the scope of application.

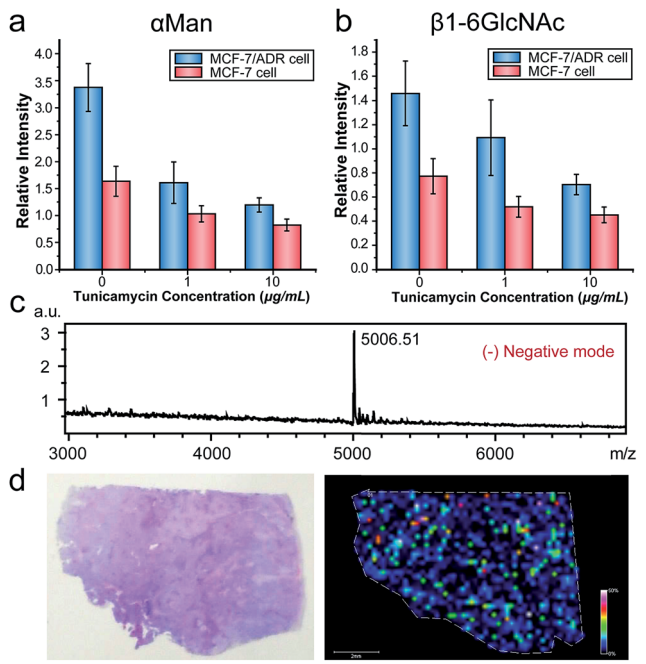

Fig. 5 Applications of the MALDI-TOF MS approach for cell surface glycan profiling. The expression alteration of (a) α-D-mannosyl groups, and (b) β1-6GlcNAc branched *N*-glycan groups in MCF-7/ADR cells and MCF-7 cells treated with TM of different concentrations for 24 h. Data are expressed as the mean of ten separate measurements ±SD. MALDI-IMS analysis of α-mannosyl groups in lung tissue: (c) overall average mass spectrum of the imaged region, and the predominant peak is *m*/*z* 5006.51; (d) optical image (left) and mass spectrometric heat map (right) of DNA probe1 (*m*/*z* = 5006.51) acquired in the tissue section. The scale bar is 2 mm.

Conclusions

In summary, we have developed a novel MALDI-TOF MS based approach for the multiplexed profiling of cell surface glycans. Based on DNA-mediated cell surface engineering, glycan groups are *in situ* profiled with high sensitivity and specificity. Diverse DNA design facilitates a multiplexed analysis, with unlimited mass tags. The DNA amplification procedure improves the sensitivity, which is suitable for low abundance glycan analysis. This approach has been successfully applied to profile the glycomic alterations in breast cancer cell lines. It was also utilized in MALDI-IMS, providing the intrinsic distribution of glycans in tissue sections. For further application, this approach can be extended to analyze cellular proteins, using DNA conjugated antibodies, as demonstrated in Fig. S9.† This multiplexed, high-sensitive and versatile method provides new insights into biomarker analysis, and contributes to the development of clinical diagnostics.

Acknowledgements

This work was financially supported by National Natural Science Foundation of China (No. 21435002, 81373373, 21227006).

References

1 J. F. Rakus and L. K. Mahal, *Annu. Rev. Anal. Chem.*, 2011, **4**, 367–392.
2 K. W. Moremen, M. Tiemeyer and A. V. Nairn, *Nat. Rev. Mol. Cell Biol.*, 2012, **13**, 448–462.
3 K. Ohtsubo and J. D. Marth, *Cell*, 2006, **126**, 855–867.
4 D. H. Dube and C. R. Bertozzi, *Nat. Rev. Drug Discovery*, 2005, **4**, 477–488.
5 A. N. Samraj, O. M. Pearce, H. Laubli, A. N. Crittenden, A. K. Bergfeld, K. Banda, C. J. Gregg, A. E. Bingman, P. Secrest, S. L. Diaz, N. M. Varki and A. Varki, *Proc. Natl. Acad. Sci. U. S. A.*, 2015, **112**, 542–547.
6 K. Marino, J. Bones, J. J. Kattla and P. M. Rudd, *Nat. Chem. Biol.*, 2010, **6**, 713–723.
7 H. Jiang, B. P. English, R. B. Hazan, P. Wu and B. Ovryn, *Angew. Chem., Int. Ed.*, 2015, **54**, 1765–1769.
8 E. L. Bird-Lieberman, A. A. Neves, P. Lao-Sirieix, M. O'Donovan, M. Novelli, L. B. Lovat, W. S. Eng, L. K. Mahal, K. M. Brindle and R. C. Fitzgerald, *Nat. Med.*, 2012, **18**, 315–321.
9 J. Hirabayashi, M. Yamada, A. Kuno and H. Tateno, *Chem. Soc. Rev.*, 2013, **42**, 4443–4458.
10 T. Bertok, L. Klukova, A. Sediva, P. Kasak, V. Semak, M. Micusik, M. Omastova, L. Chovanova, M. Vlcek, R. Imrich, A. Vikartovska and J. Tkac, *Anal. Chem.*, 2013, **85**, 7324–7332.
11 Y. W. Zhang, M. Z. Zhao, J. X. Liu, Y. L. Zhou and X. X. Zhang, *J. Sep. Sci.*, 2015, **38**, 475–482.
12 M. J. Kailemia, L. R. Ruhaak, C. B. Lebrilla and I. J. Amster, *Anal. Chem.*, 2014, **86**, 196–212.
13 W. Morelle and J. C. Michalski, *Nat. Protoc.*, 2007, **2**, 1585–1602.
14 T. W. Powers, E. E. Jones, L. R. Betesh, P. R. Romano, P. Gao, J. A. Copland, A. S. Mehta and R. R. Drake, *Anal. Chem.*, 2013, **85**, 9799–9806.
15 C. Dai, L. H. Cazares, L. Wang, Y. Chu, S. L. Wang, D. A. Troyer, O. J. Semmes, R. R. Drake and B. Wang, *Chem. Commun.*, 2011, **47**, 10338–10340.
16 H.-J. Gabius, S. André, J. Jiménez-Barbero, A. Romero and D. Solís, *Trends Biochem. Sci.*, 2011, **36**, 298–313.
17 W. Zhao, M. M. Ali, M. A. Brook and Y. Li, *Angew. Chem., Int. Ed.*, 2008, **47**, 6330–6337.
18 R. C. Bailey, G. A. Kwong, C. G. Radu, O. N. Witte and J. R. Heath, *J. Am. Chem. Soc.*, 2007, **129**, 1959–1967.
19 M. W. Duncan, H. Roder and S. W. Hunsucker, *Briefings Funct. Genomics Proteomics*, 2008, **7**, 355–370.
20 C. F. Higgins, *Nature*, 2007, **446**, 749–757.
21 H. Ma, L. Cheng, K. Hao, Y. Li, X. Song, H. Zhou and L. Jia, *PLoS One*, 2014, **9**, e85113.
22 A. D. Elbein, *Annu. Rev. Biochem.*, 1987, **56**, 497–534.
23 D. A. Greer and S. Ivey, *Biochim. Biophys. Acta*, 2007, **1770**, 1275–1282.
24 J. C. M. De-Freitas, L. G. Bastos, C. A. Freire-Neto, B. Du Rocher, E. S. F. W. Abdelhay and J. A. Morgado-Diaz, *J. Cell. Biochem.*, 2012, **113**, 2957–2966.